

Solvothermal preparation and tribological performance of g-C₃N₄/TiO₂ hybrids as oil-based lubricant additives

Feixia Zhang^{1,2}, Guogang Tang² ✉, Jin Xu¹, Changsheng Li¹ ✉

¹School of Materials Science and Engineering, Jiangsu University, Zhenjiang, Jiangsu province 212013, People's Republic of China

²School of Modern Equipment Manufacturing, Zhenjiang College, Zhenjiang, Jiangsu province 212028, People's Republic of China

✉ E-mail: g_tang78@hotmail.com; lichangsheng2008@yahoo.com.cn

Published in Micro & Nano Letters; Received on 12th April 2019; Revised on 22nd August 2019; Accepted on 18th September 2019

TiO₂ nanospheres wrapped by graphene-like g-C₃N₄ nanosheets were fabricated through the one-pot solvothermal process and applied as lubricant additives in paraffin base oil to characterise the tribology performances. Moreover, g-C₃N₄/TiO₂ composites were investigated by different characterisation methods such as X-ray diffraction, X-ray photoelectron spectroscopy, and transmission electron microscopy, indicating the formation of g-C₃N₄/TiO₂ composites. Subsequently, the friction experiment of the resulting samples using g-C₃N₄/TiO₂ hybrids as additives in base oil were tested by a multispecimen friction and wear tester (UMT-2), which indicate g-C₃N₄/TiO₂ composites possessed excellent tribological property including significantly reduced frictional coefficient and wear rate as an oil additive, owing to the presence of a thin physical lubricating film on the surface of the matrix.

1. Introduction: Nowadays, friction and wear have been widely considered as parasitic events in daily production, which leads to energy and material losses and shorter life of mechanical parts and equipment. Therefore, friction reduction and wear resistance are still one of the biggest challenges for the demands in the fields of energy and environment [1–3]. More importantly, more recent worldwide joint efforts commit to design and develop novel multifunctional lubricant nanomaterials due to their high efficiency, low cost and environmental friendly [4, 5].

Essentially, the relevant research of lubricant nanomaterials is contributed to proffer evidently enhanced efficiencies in the regeneration and recycling of energy, and also one of the most basic demands of society. Recently, lamellar materials with two-dimensional (2D) structures such as carbon-based nanomaterials (graphene, g-C₃N₄ etc.) [3, 6, 7], hexagonal boron lamellar materials nitride [5, 8, 9], lamellar metal sulphide (e.g. MoS₂ and NbS₂) [10–12], has been recognised as effective lubricating materials because of their easy interlaminar slip ascribed to the comparatively weak van der Waals intermolecular force. For example, graphene and its derivatives, as an exciting new material, have been widely studied for their friction and wear properties as self-lubricating solids, surface coating, composites, and as additives in grease and/or liquid lubricants (e.g. oils or water). Recently, graphene-like materials have been authenticated as ideal substrates to load metal or ceramic nanoparticles, such as nanometre Au, Ag, SiC, Al₂O₃, and TiO₂ [13–16], which can effectively improve their tribological properties owing to their low surface energy and high loading capacity. Moreover, many previous investigations of TiO₂ nanomaterials with various morphologies also indicated that they provide good friction reduction and excellent antiwear properties [17–20]. In this review, the above previous works could provide an effective synthesis strategy of TiO₂ coupled with 2D materials with enhanced their tribological properties.

Similarly, graphene-like carbon nitride (g-C₃N₄) with special 2D structure, was also considered to possess good tribological properties in preparation for composite and has been one of the best candidates for lubricant due to excellent thermal stability, hydrothermal stability and layered structure [21–24]. However, the tribological properties of g-C₃N₄ and its composites have been less reported, which can be widely applied in photocatalyst, electrode

material, fluorescent sensor, hydrogen storage material etc. [25–28]. Herein, g-C₃N₄/TiO₂ nanocomposite was successfully fabricated via the above synthetic methods and applied as lubricant additives in paraffin base oil to characterise the tribology performances, and the results also indicate g-C₃N₄/TiO₂ exhibited excellent friction and wear properties with the lower friction coefficient and wear rate compared with base oil. As far as we know, it was the first report on applying in lubrication field using g-C₃N₄/TiO₂ hybrids as a lubricant additive added to the base oil.

2. Experimental section

2.1. Solid-state synthesis of g-C₃N₄ nanosheets: All chemical reagents were of analytic purity from the Sinopharm Chemical Reagent Co., Ltd and used directly without further purification.

Many previous reports provide a mature approach of solid-state sintering to synthesise graphitic g-C₃N₄ with sheet-like nanostructure using urea as a precursor [29]. In the solid-state reaction process, urea powder (5 g) was added to a quartz crucible and heated to 520°C in a muffle furnace for 3 h (at 10°C min⁻¹). After cooling down to room temperature, the g-C₃N₄ powder was collected and grounded into powders for further use.

2.2. Solvothermal synthesis of g-C₃N₄/TiO₂ composites: The g-C₃N₄/TiO₂ composites were fabricated through a one-pot solvothermal approach in the tetrabutyl titanate (TBOT)–acetic acid (HAc) system [27], as illustrated in Fig. 1. Typically, 0.1 g g-C₃N₄ nanosheets were added to 50 ml HAc solution with continuous ultrasound dispersion for 60 min. After that, 1.5 ml TBOT was added gradually to the above solution with continuous stirring for 60 min, and then further transferred to a Teflon-lined autoclave (100) ml and kept at 220°C for 16 h. After the autoclave cooled to room temperature, the as-prepared products were collected by centrifugation, and washed three times with deionised water and absolute ethanol, and dried at 60°C in vacuum for 10 h. For the sake of contrast, pure TiO₂ nanospheres were prepared using a similar method without adding g-C₃N₄ nanosheets.

2.3. Structural characterisation of the samples: The material phase composition of the as-synthesised products was investigated by X-ray diffraction (XRD) on a D8 advance (Bruker-AXS)

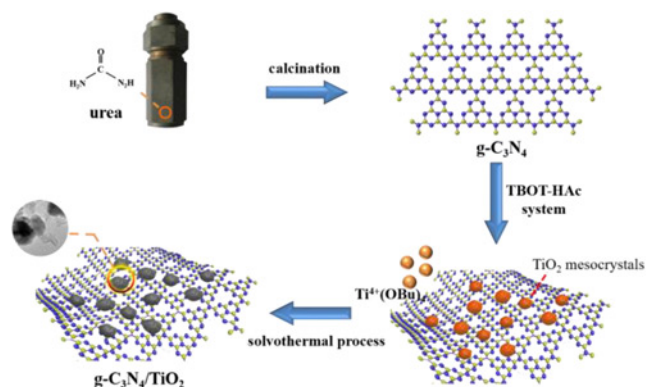


Fig. 1 Schematic illustration of the synthesis of $g\text{-C}_3\text{N}_4/\text{TiO}_2$ nanocomposites

diffractometer with Cu $K\alpha$ radiation ($\lambda = 0.1546$ nm) radiation source. The morphologies and structures of the above lubrication were detected by transmission electron microscopy (TEM, JEM-100CX II, Japan) at an accelerating voltage of 100 kV. X-ray photoelectron spectroscopy (XPS) was measured by a PHI ESCA-5000C electron spectrometer (Al $K\alpha$, 150 W, C 1 s 284.8 eV) aiming at making a better sense of chemical states of various samples.

2.4. Preparation of lubricating oil samples and tribological experiment: The paraffin oil sample with adding $g\text{-C}_3\text{N}_4/\text{TiO}_2$ composites was dispersed by monooleate (Span-80) with continuous ultrasonication for 30 min. The additive concentration of $g\text{-C}_3\text{N}_4/\text{TiO}_2$ is 0.5, 1, 3, and 5 wt%, respectively. The friction experiment of the resultant samples using $g\text{-C}_3\text{N}_4/\text{TiO}_2$ composites as additives in base oil was examined by a multi-specimen friction and wear tester (UMT-2) under the condition of different load (10–60 N) with steady speed (50 rpm) or various rotational speed (50–400) rpm with constant load (10 N) for 60 min. The UMT-2 tester adopts ball-on-disk construction consisted of 440C stainless steel ball (\varnothing 10 mm, 62 HRC) and 45 steel disc (\varnothing 40 mm \times 3 mm). Moreover, each friction experiment was measured and tested three times to acquire the average value of the friction coefficient and wear rate of the oil samples. Also, the topographic images of the worn steel surfaces were investigated using a scanning electron microscope (SEM, HITACHI S-3400 N, Japan) and non-contact optical 3D profilers (SMP, NT1100, Veeco WYKO, USA) after a tribological experiment. For comparison, the tribological performances of pure $g\text{-C}_3\text{N}_4$ and TiO_2 particles using additives in paraffin oil were also measured under the same conditions.

3. Results and discussion: Fig. 2 shows the XRD patterns of three samples involved pure $g\text{-C}_3\text{N}_4$, TiO_2 , and $g\text{-C}_3\text{N}_4/\text{TiO}_2$, clearly, there are two characteristic peaks ($2\theta = 27.8^\circ$ and 13.3°) in the XRD patterns of $g\text{-C}_3\text{N}_4$, corresponding to (002) and (100) planes of standard photographs JCPDF 87–1526 of $g\text{-C}_3\text{N}_4$. In addition, all diffraction peaks of TiO_2 is consistent with that of anatase TiO_2 (JCPDS Card No. 21-1272), which is consistent with previous references [30, 31]. Furthermore, the presence of characteristic peaks of $g\text{-C}_3\text{N}_4$ and TiO_2 in the $g\text{-C}_3\text{N}_4/\text{TiO}_2$ system can be easily obtained simultaneously [32, 33]. Moreover, no other impurity substance was detected, suggesting that TiO_2 is well combined with $g\text{-C}_3\text{N}_4$ with high chemical purity. Further to verify the chemical status of the above samples, XPS was conducted on the obtained $g\text{-C}_3\text{N}_4/\text{TiO}_2$, as shown Fig. 3. According to the XPS observations, $g\text{-C}_3\text{N}_4/\text{TiO}_2$ composites contained C 1s, N 1s, Ti 2p and O 1s (Fig. 3a). Obviously, there are three peaks centring at 284.6, 285.88, and 288.12 eV in the

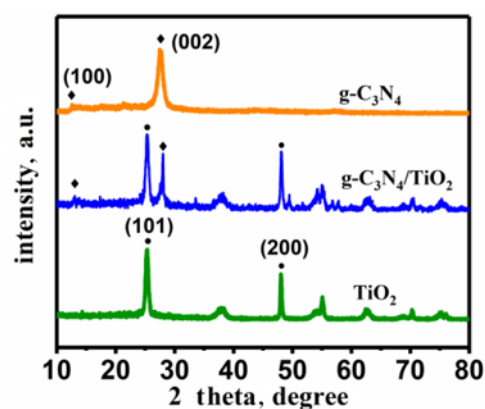


Fig. 2 XRD patterns of the as-prepared $g\text{-C}_3\text{N}_4$, TiO_2 , and $g\text{-C}_3\text{N}_4/\text{TiO}_2$ hybrids

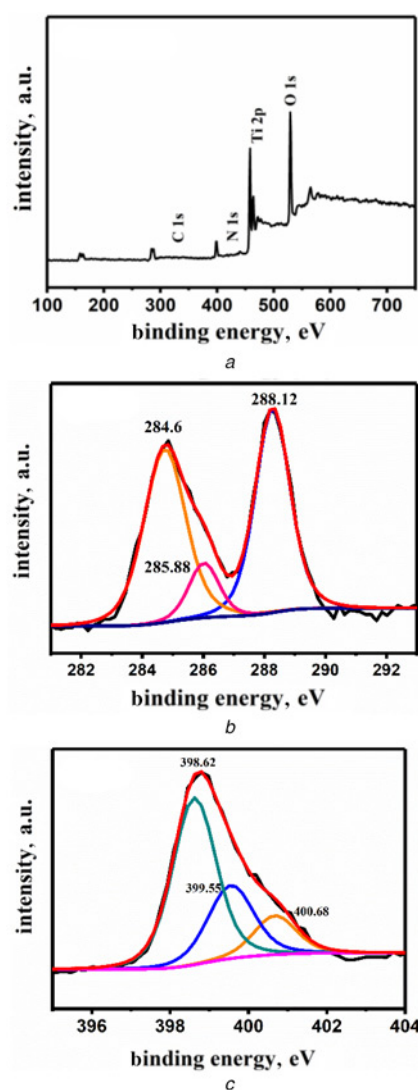


Fig. 3 XPS spectra of the as-prepared $g\text{-C}_3\text{N}_4/\text{TiO}_2$ hybrids
a Survey spectrum
b C 1s
c N 1s

high-resolution XPS spectra of C 1s (Fig. 3b), which according to C–C coordination sp^2 bonding carbon atoms and sp^3 -hybridized orbitals N=C=N present in $g\text{-C}_3\text{N}_4$. Moreover, the high-resolution

spectrum of N 1s (Fig. 3c) is split into three peaks located at 398.62, 399.55 and 400.68 eV, which belongs to C=N–C, N–(C)₃ and C–N–H groups [32–34], separately. Therefore, XPS data together with those from the XRD can be concluded the fabrication of binary system g-C₃N₄/TiO₂.

The surface micrographs and structure of the as-prepared products including pure g-C₃N₄, TiO₂, and g-C₃N₄/TiO₂ composites were investigated by TEM, as demonstrated in Fig. 4. In comparison, the TEM image of graphitic g-C₃N₄ is described in Fig. 4a, indicating g-C₃N₄ possesses a typical lamellar structure with non-uniform diameters and the surfaces are very smooth. Fig. 4b shows the uniform sphere-like morphology of TiO₂ particles with average diameter of 300 nm. As shown in Fig. 4c, lamellar g-C₃N₄ is well coated TiO₂ nanospheres with ~200–500 nm in diameter, which densely and evenly anchor on the nanosheets' surface. Furthermore, energy dispersive X-ray (EDX) analysis was performed to investigate the composition of g-C₃N₄/TiO₂ composites (Fig. 4d), where the appeared peaks confirmed that the product was only composed of C, N, O, and Ti elements, further indicating the formation of g-C₃N₄/TiO₂ heterostructures.

The friction and wear behaviours of pure g-C₃N₄, TiO₂, and g-C₃N₄/TiO₂ composites were tested using a ball-on-plate tribometer. Also, the tribological test was performed using paraffin contained with 1 wt% lube additives under the condition of constant load (10 N) and steady speed (50 rpm) and continuous operation for 60 min. Clearly, a steady variation curve of friction coefficient and time of paraffin oil containing g-C₃N₄/TiO₂ were observed from Fig. 5a, which indicated the above tribological experiment is a stable friction-reducing process with addition of g-C₃N₄/TiO₂ additive. More importantly, the friction coefficient of paraffin with g-C₃N₄, TiO₂, and g-C₃N₄/TiO₂ are remarkably decreased

compared with pure paraffin. Meanwhile, the tendency of the wear rate of all lube additives is similar to that of friction coefficient (Fig. 5b). Furthermore, the coefficient of frictions (COFs) of liquid paraffin contained with different amount of g-C₃N₄/TiO₂ (0.5, 1, 3, and 5 wt%) was investigated under the same conditions (load = 5 N, speed = 50 rpm, time = 30 min), resulted in Fig. 5c. Clearly, g-C₃N₄/TiO₂ composites exhibit the minimum COF (~0.08) among all oil additives, which can effectively improve the friction properties of liquid paraffin. Additionally, the wear rate of all oil samples contained with g-C₃N₄/TiO₂ shows the similar tendency of COFs (Fig. 5d), which also show the minimum wear rate ($4.05 \times 10^{-5} \text{ mm}^3/\text{Nm}$) with 1% g-C₃N₄/TiO₂ as lubricant additives in pure paraffin. Moreover, the tribological tests were further investigated under the condition of different load with steady speed (50 rpm) or various rotational speeds with constant load (10 N) for 60 min, as shown in Fig. 6. For all four samples, the friction coefficients of paraffin oil contained with various additives are lower, compared with that of pure paraffin oil with the load increasing (10, 20, 40, and 60 N), as shown Fig. 6a. Especially, the paraffin oil with g-C₃N₄/TiO₂ composite was reduced remarkably and stabilised compared with other additives at higher load. Similarly, the lubricant of g-C₃N₄/TiO₂ composite in base oil reveals supreme tribological properties compared as pure g-C₃N₄ or TiO₂ at different rotating speeds including 50, 100, 200, and 400 rpm (Fig. 6b). Therefore, g-C₃N₄/TiO₂ composite possessed improved antifriction and antiwear property of the matrix material.

To further study the tribological performances of g-C₃N₄/TiO₂ composite, topographic images of the worn steel surfaces were investigated using a SEM and non-contact 3D optical profilers (SMP) after rubbing surfaces under the condition of constant load (10 N) and steady speed (50 rpm) and continuous operation for

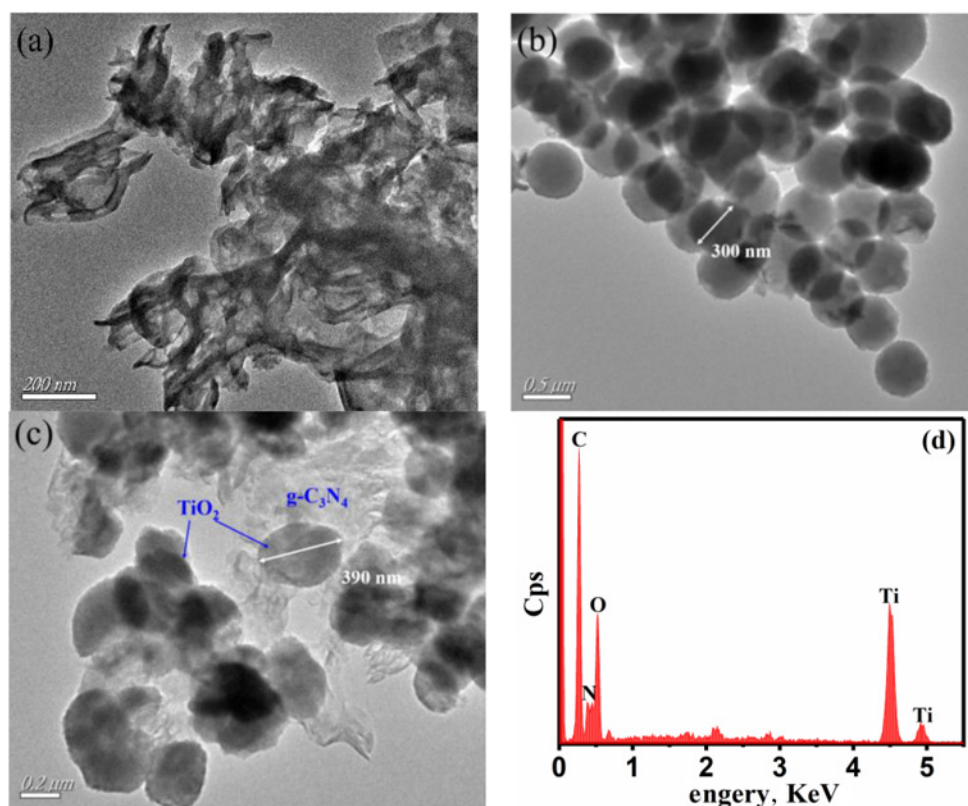


Fig. 4 TEM image of
a g-C₃N₄,
b TiO₂
c g-C₃N₄/TiO₂ composites
d EDX analysis of g-C₃N₄/TiO₂ composites

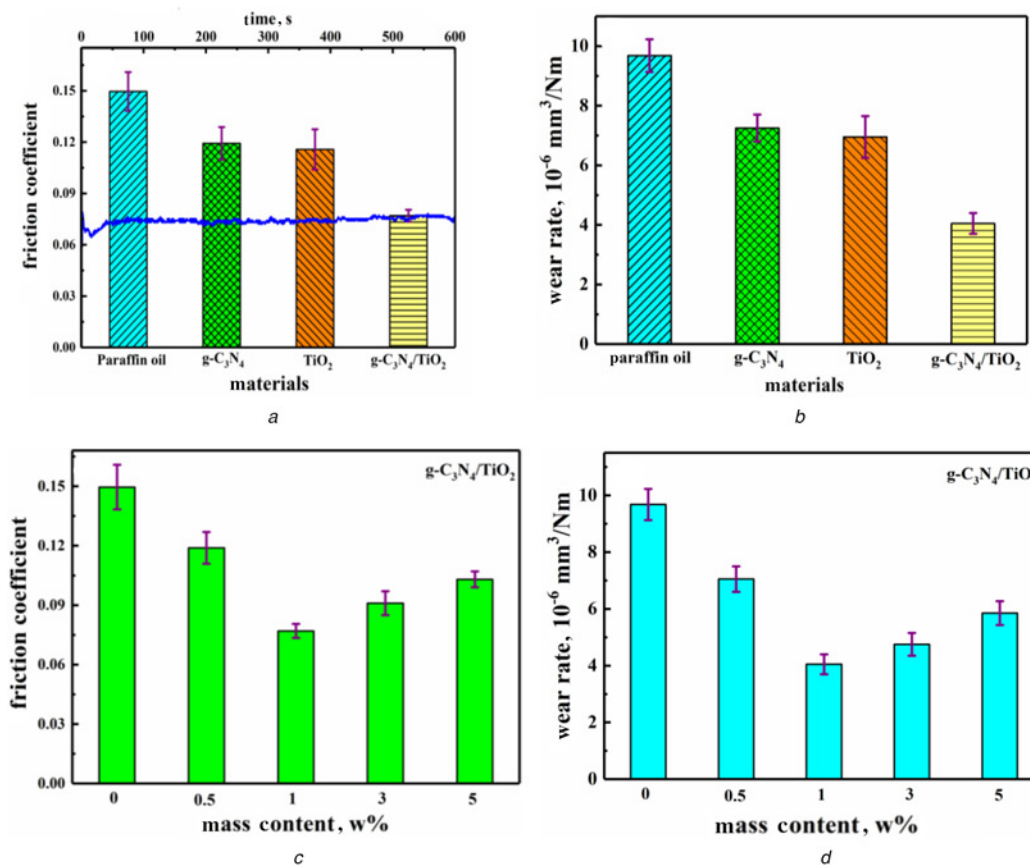


Fig. 5 Tribological properties of the as-prepared g-C₃N₄/TiO₂ for improved base oil

a Mean friction coefficients

b Mean wear rates of base oil with different additives (paraffin oil and g-C₃N₄, TiO₂, and g-C₃N₄/TiO₂ additives) at 50 rpm under 10 N loads for 1 h. The inset line shows changes in the friction coefficient relative to time under the same conditions for paraffin contained with C₃N₄/TiO₂

c Friction coefficient

d Wear rate of liquid paraffin contained with different g-C₃N₄/TiO₂ additive

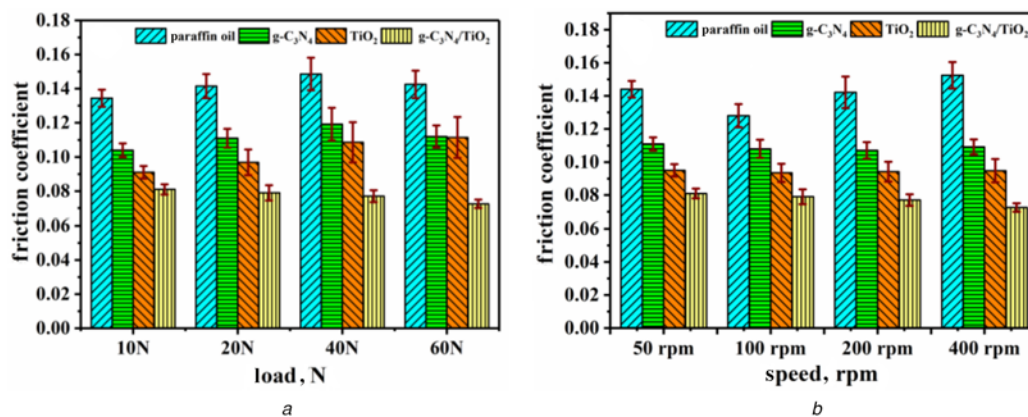


Fig. 6 Variations of the mean friction coefficient of paraffin with different additives

a Increasing load (10, 20, 40, and 60 N),

b Under diverse speeds (50, 100, 200, and 400 rpm)

60 min. Obviously, the friction surfaces lubricated by paraffin oil have several wider and deeper furrows, as shown in Fig. 7a, while only represented slender furrows were obtained in steel pans lubricated with g-C₃N₄/TiO₂ composites (Fig. 7b). Analogously, it can be observed from Figs. 7c and d that the grinding crack on the surface of steel pans lubricated by paraffin oil with 1.0 wt% g-C₃N₄/TiO₂ composite is shallower and sparser compared with that caused by pure paraffin. Meanwhile, the wear scar depth

and width of paraffin oil with the addition of g-C₃N₄/TiO₂ composite (Fig. 7c) are about 2.18 and 205.7 μm , and those lubricated by paraffin oil (Fig. 7d) are about 3.74 and 278.1 μm , respectively. The above results also prove paraffin oil containing g-C₃N₄/TiO₂ composite had the excellent anti-wear property.

Based on the above experimental results and in the previous literature, the enhanced tribological performance was attributed to the synergistic interaction of g-C₃N₄ and TiO₂. On the one hand,

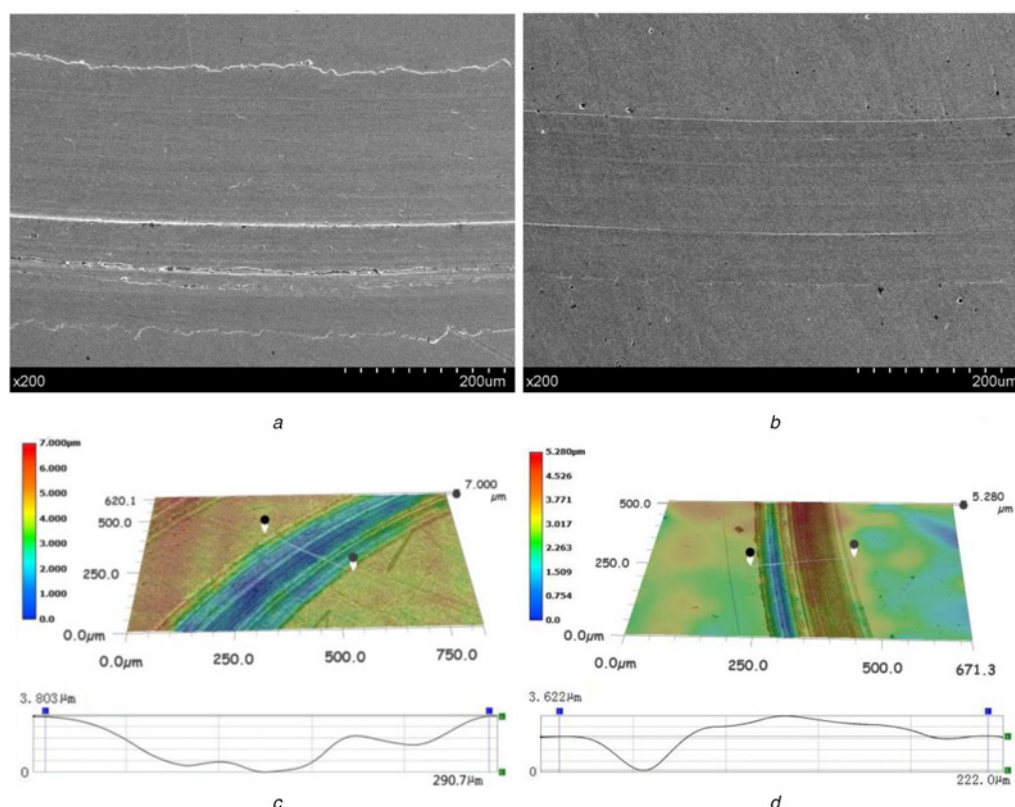


Fig. 7 SEM images of non-contact 3D images of wear scar at 50 rpm under 10 N loads for 1 h
 a, c Pure oil paraffin
 b, d Paraffin contained with g-C₃N₄/TiO₂ composites

g-C₃N₄/TiO₂ nanoparticles can easily penetrate into the interface with a base oil, strongly adhere to substrates and form continuous film in concave of rubbing surface, which hindered the direct contact between the interfaces of steel disc and ball [35, 36]. On the other hand, the rolling friction plays a leading role in the friction process with the addition of TiO₂ nanospheres. Moreover, TiO₂ nanospheres can easily form micro-polishing effects in the friction pair, acting like no-ball bearings [37, 38], thus effectively decreasing the COFs of pure oil. Therefore, oil-g-C₃N₄/TiO₂ system consisted of layered g-C₃N₄ and sphere-like TiO₂ show excellent tribological properties due to their unique structure and synergistic interaction.

4. Conclusions: In summary, graphitic g-C₃N₄ nanosheets couple with TiO₂ nanospheres of ~200–500 nm in diameter prepared through a facile and effective one-pot solvothermal process and applied as base oil additives to investigate the tribological properties. Moreover, preliminary tribological tests indicate g-C₃N₄/TiO₂ composite mixed with paraffin oil exhibited superior friction reduction and antiwear properties compared with pure paraffin oil. Moreover, the excellent performance of g-C₃N₄/TiO₂ composites with improved tribological properties of paraffin oil is mainly accredited to the lubricated synergism of frictional couple between g-C₃N₄ and TiO₂ on the interface.

5. Acknowledgments: This work was financially supported by the China Postdoctoral Science Foundation (grant nos. 2017M611733 and 2017M611715), the Natural Science Foundation of Jiangsu Higher Education Institutions of China (grant no. 17KJB30012), the High-end Research Project of Jiangsu Higher Vocational Education Institutions (grant no. 2018TDFX010) and the Primary Research & Development Plan (social development project) of Zhenjiang (grant no. SH2017059), and G.T. gratefully

acknowledges financial support from the second batch of scientific research team of Zhenjiang College.

6 References

- [1] Paul G., Hirani H., Kuila T., *ET AL.*: 'Nanolubricants dispersed with graphene and its derivatives: an assessment and review of the tribological performance', *Nanoscale*, 2019, **2019**, (11), pp. 3458–3483
- [2] Li Y., Wang Q., Wang S.: 'A review on enhancement of mechanical and tribological properties of polymer composites reinforced by carbon nanotubes and graphene sheet: molecular dynamics simulations', *Compos. B. Eng.*, 2018, **160**, pp. 348–361
- [3] Miranzo P., Belmonte M., Osendi M.I.: 'From bulk to cellular structures: a review on ceramic/graphene filler composites', *J. Eur. Ceram. Soc.*, 2017, **37**, (12), pp. 3649–3672
- [4] Furlan K.P., de Mello J.D.B., Klein A.N.: 'Self-lubricating composites containing MoS₂: a review', *Tribol. Int.*, 2018, **120**, pp. 280–298
- [5] Yu J., Zhao W., Wu Y., *ET AL.*: 'Tribological properties of epoxy composite coatings reinforced with functionalized C-BN and H-BN nanofillers', *Appl. Surf. Sci.*, 2018, **434**, pp. 1311–1320
- [6] Sharma A.K., Tiwari A.K., Dixit A.R., *ET AL.*: 'Novel uses of alumina/graphene hybrid nanoparticle additives for improved tribological properties of lubricant in turning operation', *Tribol. Int.*, 2018, **119**, pp. 99–111
- [7] Sanes J., Avilés M.D., Saurín N., *ET AL.*: 'Synergy between graphene and ionic liquid lubricant additives', *Tribol. Int.*, 2017, **116**, pp. 371–382
- [8] Charoo M.S., Wani M.F.: 'Tribological properties of h-BN nanoparticles as lubricant additive on cylinder liner and piston ring', *Lubr. Sci.*, 2017, **29**, (4), pp. 241–254
- [9] Podgornik B., Kafexhiu F., Kosec T., *ET AL.*: 'Friction and anti-galling properties of hexagonal boron nitride (h-BN) in aluminium forming', *Wear*, 2017, **388**, pp. 2–8
- [10] Fang L., Liu D.M., Guo Y., *ET AL.*: 'Thickness dependent friction on few-layer MoS₂, WS₂, and WSe₂', *Nanotechnology*, 2017, **28**, (24), p. 245703

- [11] Domínguez-Meister S., Rojas T.C., Brizuela M., *ET AL.*: 'Solid lubricant behavior of MoS₂ and WSe₂-based nanocomposite coatings', *Sci. Technol. Adv. Mater.*, 2017, **18**, (1), pp. 122–133
- [12] Tang G., Zhang J., Liu C., *ET AL.*: 'Synthesis and tribological properties of flower-like MoS₂ microspheres', *Ceram. Int.*, 2014, **40**, (8), pp. 11575–11580
- [13] Meng Y., Su F., Chen Y.: 'Au/graphene oxide nanocomposite synthesized in supercritical CO₂ fluid as energy efficient lubricant additive', *ACS Appl. Mater. Interfaces*, 2017, **9**, (45), pp. 39549–39559
- [14] Liu X., Shi X., Huang Y., *ET AL.*: 'Tribological behavior of TiAl-multilayer graphene-silver composites at different sliding speeds', *Mater. Chem. Phys.*, 2018, **213**, pp. 368–373
- [15] Yuan Z., He Y., Cheng K., *ET AL.*: 'Effect of self-developed graphene lubricant on tribological behaviour of silicon carbide/silicon nitride interface', *Ceram. Int.*, 2019, **45**, (8), pp. 10211–10222
- [16] Du S., Sun J., Wu P.: 'Preparation, characterization and lubrication performances of graphene oxide–TiO₂ nanofluid in rolling strips', *Carbon*, 2018, **140**, pp. 338–351
- [17] Wu H., Zhao J., Xia W., *ET AL.*: 'A study of the tribological behaviour of TiO₂ nano-additive water-based lubricants', *Tribol. Int.*, 2017, **109**, pp. 398–408
- [18] Kong L., Sun J., Bao Y., *ET AL.*: 'Effect of TiO₂ nanoparticles on wettability and tribological performance of aqueous suspension', *Wear*, 2017, **376**, pp. 786–791
- [19] Yoon Y., Park J.: 'The effects of nanostructures on the mechanical and tribological properties of TiO₂ nanotubes', *Nanotechnology*, 2018, **29**, (16), p. 165705
- [20] Tao X., Yao Z., Luo X.: 'Comparison of tribological and corrosion behaviors of Cp Ti coated with the TiO₂/graphite coating and nitrated TiO₂/graphite coating', *J. Alloys Compd.*, 2017, **718**, pp. 126–133
- [21] Zhu L., Wang Y., Hu F., *ET AL.*: 'Structural and friction characteristics of g-C₃N₄/PVDF composites', *Appl. Surf. Sci.*, 2015, **345**, pp. 349–354
- [22] Yang J., Zhang H., Chen B., *ET AL.*: 'Fabrication of the g-C₃N₄/Cu nanocomposite and its potential for lubrication applications', *RSC Adv.*, 2015, **5**, (79), pp. 64254–64260
- [23] Zhu L., You L., Shi Z., *ET AL.*: 'An investigation on the graphitic carbon nitride reinforced polyimide composite and evaluation of its tribological properties', *J. Appl. Polym. Sci.*, 2017, **134**, (41), p. 45403
- [24] Tang G., Dong J., Wu K., *ET AL.*: 'Novel 3D flowerlike BiOCl_{0.7}Br_{0.3} microspheres coupled with graphene sheets with enhanced visible-light photocatalytic activity for the degradation of rhodamine B', *Ceram. Int.*, 2016, **42**, (5), pp. 5607–5616
- [25] Tang H., Chang S., Tang G., *ET AL.*: 'AgBr and g-C₃N₄ co-modified Ag₂CO₃ photocatalyst: a novel multi-heterostructured photocatalyst with enhanced photocatalytic activity', *Appl. Surf. Sci.*, 2017, **391**, pp. 440–448
- [26] Zeng D., Xu W., Ong W.J., *ET AL.*: 'Toward noble-metal-free visible-light-driven photocatalytic hydrogen evolution: monodisperse sub-15 nm Ni₂P nanoparticles anchored on porous g-C₃N₄ nanosheets to engineer 0D–2D heterojunction interfaces', *Appl. Catal. B*, 2018, **221**, pp. 47–55
- [27] Tang H., Chang S., Jiang L., *ET AL.*: 'Novel spindle-shaped nanoporous TiO₂ coupled graphitic g-C₃N₄ nanosheets with enhanced visible-light photocatalytic activity', *Ceram. Int.*, 2016, **42**, (16), pp. 18443–18452
- [28] Patnaik S., Sahoo D.P., Parida K.: 'An overview on Ag modified g-C₃N₄ based nanostructured materials for energy and environmental applications', *Renew. Sustain. Energy Rev.*, 2018, **82**, pp. 1297–1312
- [29] Zhang M., Xu J., Zong R.: 'Enhancement of visible light photocatalytic activities via porous structure of g-C₃N₄', *Appl. Catal. B*, 2014, **147**, pp. 229–235
- [30] Tan Y., Shu Z., Zhou J., *ET AL.*: 'One-step synthesis of nanostructured g-C₃N₄/TiO₂ composite for highly enhanced visible-light photocatalytic H₂ evolution', *Appl. Catal. B*, 2018, **230**, pp. 260–268
- [31] Li Y., Feng X., Lu Z., *ET AL.*: 'Enhanced photocatalytic H₂-production activity of C-dots modified g-C₃N₄/TiO₂ nanosheets composites', *J. Colloid Interface Sci.*, 2018, **513**, pp. 866–876
- [32] Jiang G., Geng K., Wu Y., *ET AL.*: 'High photocatalytic performance of ruthenium complexes sensitizing g-C₃N₄/TiO₂ hybrid in visible light irradiation', *Appl. Catal. B*, 2018, **227**, pp. 366–375
- [33] Li C., Lou Z., Yang Y., *ET AL.*: 'Hollowsphere nanoheterojunction of g-C₃N₄@TiO₂ with high visible light photocatalytic property', *Langmuir*, 2019, **35**, (3), pp. 779–786
- [34] Zong H., Zhao T., Zhou G., *ET AL.*: 'Revisiting structural and photocatalytic properties of g-C₃N₄/TiO₂: is surface modification of TiO₂ by calcination with urea an effective route to 'solar' photocatalyst', *Catal. Today*, 2019, **335**, pp. 252–261
- [35] Duan C., Yuan D., Yang Z., *ET AL.*: 'High wear-resistant performance of thermosetting polyimide reinforced by graphitic carbon nitride (g-C₃N₄) under high temperature', *Compos. A, Appl. Sci. Manuf.*, 2018, **113**, pp. 200–208
- [36] Wu L., Zhang Z., Yang M., *ET AL.*: 'One-step synthesis of g-C₃N₄ nanosheets to improve tribological properties of phenolic coating', *Tribol. Int.*, 2019, **132**, pp. 221–227
- [37] Wu L., Zhang Z., Yang M., *ET AL.*: 'Facile synthesis of CuO/g-C₃N₄ hybrids for enhancing the wear resistance of polyimide composite', *Eur. Polym. J.*, 2019, **116**, pp. 463–470
- [38] Deshpande P., Minfray C., Dassenoy F., *ET AL.*: 'Tribological behaviour of TiO₂ atmospheric plasma spray (APS) coating under mixed and boundary lubrication conditions in presence of oil containing MoDTC', *Tribol. Int.*, 2018, **118**, pp. 273–286